Distribution of brain sodium long and short relaxation times and concentrations: a multi-echo ultra-high field 23Na MRI study

Authors: Ben Ridley*[1,2], Armin M. Nagel[3,4], Mark Bydder[1,2], Adil Maarouf[1,2], Jan-Patrick Stellmann[1,2], Soraya Gherib[1,2], Jeremy Verneuil[1,2], Patrick Viout[1,2], Maxime Guye[1,2], Jean-Philippe Ranjeva[1,2] and Wafaa Zaaraoui[1,2] **Affiliations:** [1] Aix-Marseille Univ, CNRS CRMBM UMR 7339, Marseille, France ; [2] APHM, Hôpitaux de la Timone, CEMEREM, Marseille, France; [3] University Hospital Erlangen, Institute of Radiology, Erlangen, Germany; [4] Division of Medical Physics in Radiology, German Cancer Research Centre (DKFZ), Heidelberg, Germany

TARGET AUDIENCE: MR physicists; Neuroscientists; Neurologists

PURPOSE: Sodium ion transmembrane homeostasis is a precondition for several critical neuronal functions, subject to pathological modification as shown by ^{23}Na-MRI methods including ultra-short echo times (UTE, ~0.2ms), multiple quantum filtering (MQF) or inversion recovery (IR) [1]. However, uncertainty can arise in *in vivo* ^{23}Na estimates from signal losses given the rapidity of T2* decay given biexponential relaxation with both short ($T2^*_{short}$) and long ($T2^*_{long}$) components. Existing approaches attempt to minimise uncertainty but are insensible to different compartments (UTE), or weight toward rapidly relaxing components but suffer from strong SNR and resolution penalties (MQF), or are not easily amenable to providing quantitative estimates of sodium (IR). In contrast, we build on previous work by characterising the decay curve directly via multi-echo imaging with the requisite number, distribution and range to assess the distribution of both[2,3] *in vivo* $T_2^*_{short}$ and $T_2^*_{long}$ and in variation between grey (GM) and white matter (WM) and subregions for the first time[4,5]. Furthermore, by modelling the relationship between signal and reference concentration and applying it to *in vivo* ^{23}Na-MRI signal, we quantify Na concentrations associated with short and long components for the first time.

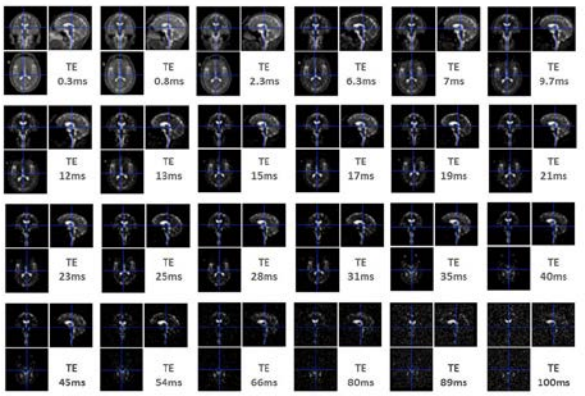

Figure 1– ^{23}Na-MRI images from a single subject across echo times.

METHODS: ^{23}Na-MRI from 13 healthy subjects was acquired at 7T using a multi-echo (24 TEs, 0.3 ms-100 ms (**Figure 1**)) density adapted 3D projection reconstruction pulse sequence (TR=120 ms, 10000 spokes, 3.5mm^3 resolution, 60 mins). Six tubes of 2% agar gel doped with a range of sodium concentrations (10-75 mM) were arrayed in the FOV. A high-resolution ^{1}H MRI 3D-MP2RAGE (TR=5000ms / TE=3ms / TI1=900ms / TI2=2750ms, 256 slices, 0.6mm^3 isotropic resolution, 10 mins) was used to define subject masks for GM, WM (SPM12, 0.9 tissue probability threshold) and 8 manually-defined regional ROIs (FSL 6.0). A biexponential fitting procedure was applied to the images of different TE derived from each individual to obtain $T_2^*_{short}$ and $T_2^*_{long}$ relaxation times for each ROI (**Figure 2a**). We measured M0 and the time of transverse relaxation (T_2*) for a given reference tube across the 24 TEs, through monoexponential fitting via MATLAB (R2012a, MathWorks), and modelled a linear relationship between obtained M0 and known concentrations across all tubes (**Figure 2b,c**). Applying this to parameters estimated from the biexponential model of *in vivo* data, yielded quantitative estimates (Na_{SF} and Na_{LF}) for each brain ROI. To permit literature comparisons, total sodium concentrations (TSC) and extracellular fractions (EcF) were also calculated. Two ANOVAs (JMP v.9) were applied to investigate factors of interest Tissue Type (2 levels: GM, WM) and Region (8 levels), in addition to Sex and Age. Factors of interest were further investigated via non-parametric Steel-Dwass tests.

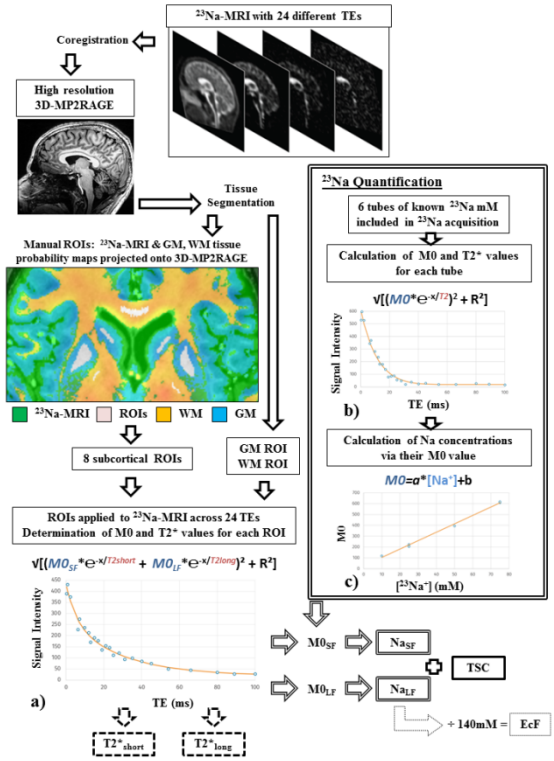

Figure 2 – Schematic workflow of processing procedure applied to data and the six measures obtained. SF, short fraction; LF, long fraction.

RESULTS: Effect of Tissue type was significant (P<0.008) for all parameters except Na_{SF} while post-hoc tests (**Figure 3a**) reveal relative levels GM>WM for Na_{LF}, $T_2^*_{short}$, extracellular fraction and TSC and WM>GM for $T_2^*_{long}$. Effect of Region was significant (P<0.008) for all parameters, and a significant effect of Sex was also observed for TSC. Overall, post-hoc (**Figure 3b**) tests revealed substantial variation for each parameter between subcortical regions, in addition to wide distributions between subjects for certain structures (especially centrum semiovale and corpus callosum) for certain parameters ($T_2^*_{long}$, EcF).

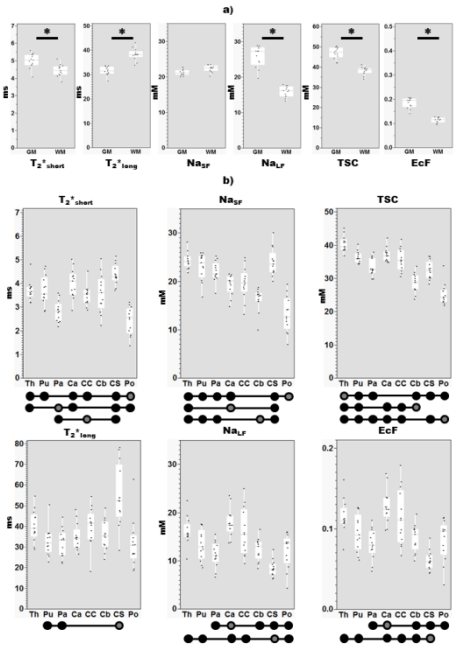

Figure 3 – Post-hoc differences (z, Steel-dwass, *P*<0.008) for a) data from whole GM, WM masks and b) sub-regions: differences between a region (circle with dark grey interior) with other regions (full black circles) are indicated below each graph. *Regions:* Th, thalamus; Pu, putamen; Pa, pallidum; Ca, caudate; Cc, corpus callosum; Cb, cerebellar WM, Cs, centrum semiovale; Po, pons.

DISCUSSION: The current data suggest that GM & WM give rise to different time constants of decay, which, given regional variation, may reflect the influence of tissue composition on observed relaxation. This would be consistent with relative observed differences in fluid content[6–8] and tissue density including the distribution, relative density and structure of neuronal and glial subtypes[9–12] influencing the volume of intra-/extracellular spaces[13]. For example, a restricted sodium pool determined mainly by the highly anisotropic[14] axonal environment and small-bodied[15] oligodendrocytes in WM, versus a wider variety of cellular environments in GM, could lead to shorter estimates of $T_2^*_{short}$ in WM and in axon/myelin-rich structures such as the pallidum, pons or CC. Consistency with previous estimates of EcF and TSC in GM vs WM and various regions[16–19] in controls samples, as well as 'bound' sodium estimates via ^{23}Na-MRI IR at 3T[20,21] and MQF at 7T[22,23], suggests that the current methods appropriately characterize the compartmental and overall ^{23}Na signal. Crucially, the current methods achieve this without a high SNR penalty and permit quantification.

CONCLUSION: We provide the first ^{23}Na-MRI data to address regional variation in $T_2^*_{short}$ at UHF, and to quantify the ^{23}Na concentrations associated with short and long components. This provides a foundation for investigating alterations due to disease processes and the factors underlying normal ionic homeostatic mechanisms as imaged by ^{23}Na-MRI.

REFERENCES: 1. Thulborn *NI* (2016) 2. Bartha. & Menon *MRM* (2004). 3. Fleysher *MRM*. (2009) 4. Nagel *Invest. Radiol.* (2011). 5. Blunck *MRM*. (2017). 6. Koessler *HBM* (2017). 7. Gelman *MRM*. (2001). 8. Krebs *J. Trace Elem. Med.* (2014). 9. von Bartheld *J. Comp. Neurol.* (2016). 10. Mota & Herculano-Houzel *Front. Neuroanat.* (2014). 11. Herculano-Houzel *Glia* (2014). 12. Azevedo *J. Comp. Neurol.* (2009). 13. Syková & Nicholson *Physiol. Rev.* (2008). 14. *Assaf* & Pasternak *J. Mol. Neurosci.* (2008). 15. Pelvig *Neurobiol. Aging* (2008). 16. Madelin, *Prog. Nucl. Magn. Reson. Spectrosc.* 4). 17. Inglese *Brain J. Neurol.* (2010). 18. Reetz *NI* 19. Zaaraoui *Radiology* (2012). 20. Madelin *Sci. Rep.* (2014). 21. Madelin *PloS1* (2015). 22. Petracca *Brain J. Neurol.* (2016). 23. Fleysher *NMR Biomed.* (2013).